III. *Viking* Project, Orbiter System and Project Support

A. Project Description and Status

1. Description

The primary objective of the *Viking* Project is to significantly advance the knowledge of the planet Mars by direct measurements in the atmosphere and on the surface and by observations of the planet during approach and from orbit. Particular emphasis will be placed on obtaining information concerning biological, chemical, and environmental factors relevant to the existence of life on the planet at this time, at some time in the past, or the potentials for the development of life at a future date. Two spacecraft, each consisting of an Orbiter System and a Lander System, are planned for launch during the 1975 opportunity. The Orbiter System is being developed by JPL; the Langley Research Center is responsible for the Lander System, which is being developed under contract by the Martin Marietta Corporation. Langley has overall management responsibility for the *Viking* Project.

The orbiter will transport and insert the lander into Mars orbit at the appropriate point for a given range of preselected landing areas. The topography of Mars will be mapped during orbital operations, with special emphasis on mapping proposed landing sites prior to deorbit of the lander and on supporting the lander after it is on the surface of Mars by determining if changes are apparent in the vicinity of the lander. After the lander has landed, the orbiter will relay telemetered data from the lander to earth. Scientific instruments on the orbiter will be used to measure atmospheric and surface parameters at various times and locations to determine the dynamic characteristics of the planet. Both visual and infrared coverage will be possible during the presently planned 140 days of orbital operations.

During entry the lander will measure Mars' upper atmospheric composition and lower atmospheric temperature, pressure, and density. After landing, surface soil analyses will be conducted by an integrated biology instrument to detect evidence of biological growth and/or metabolism and by a gas chromatograph/mass spectrometer to measure the molecular composition with particular emphasis on determining organic compounds. In addition, the landing site and surrounding areas will be mapped visually, and measurements will be made of the planet's atmospheric composition, temperature, pressure, humidity, and wind speed. Seismological, magnetic, and physical properties will be determined.

2. Status

All Action Items assigned to JPL at the *Viking* Project mission trade study review in July 1970 were completed.

Efforts are continuing in related areas of relay antenna capability, the impact of a fixed raster alignment (other than the baseline description), and in processing a configuration change on the orbiter from a 6-panel to a 4-panel arrangement.

Test activity on the gas chromatograph mass spectrometer engineering breadboard continued, after minor problems in wiring and cabling were disclosed and corrected during instrument data subsystem-instrument integration tests. Engineering model design continued, with the establishment of an instrument case configuration. Detail design and layout of components was started.

Detailed reviews were conducted covering the technical divisions' operating plans for the remainder of FY 1971 and the initiation of major hardware procurements in FY 1972. These reviews were conducted to identify required FY 1971 orbiter activities and the resources associated with their support.

B. Relay Link Multipath Simulation, *Spacecraft Communications Systems Section*

1. Introduction

The *Viking* relay link will operate at various times during the mission and provides the capability for lander-to-orbiter (uplink) and orbiter-to-lander (downlink) communications via a UHF channel. The uplink will be supported by a telemetry transmitter in the lander and a telemetry receiver/detector in the orbiter. Data will be transmitted through the uplink at 4.0 or 16.0 kilobits/s and is binary Manchester-coded frequency-shift-keyed. The recovered data stream may be recorded in the orbiter and, in the case of 4.0-kilobits/s data, relayed real-time to earth. The downlink will be supported by an amplitude-modulated transmitter in the orbiter and a receiver/tone detector in the lander. The orbiter may address a particular lander by means of a unique tone modulated on the downlink signal. The lander will respond with an uplink modulated with real-time data. When the orbiter has acquired the data stream, it initiates transmission of an enable tone. The lander then responds with playback of stored data. Playback will continue for a specified period of time and until the enable tone is lost, then ceases. A more comprehensive description of link operation and equipment may be found in SPS 37-63, Vol. I, pp. 54–61.

Previous flight projects have not used relay links, and design of this link represents a first effort in many areas. Accordingly, little experience is available on which to base predictions of performance. In order to ensure integrity of design, and to evaluate link parameters, a simulation program has been undertaken to duplicate link signals at various mission phases and measure actual equipment responses.

2. Background

The *Viking* relay link encounters degradation from signals reflected at the surface of the planet. Previous flyby programs have not had to account for these reflections because of the range between probe and planet and because of the highly directive antennas on the spacecraft. With *Viking*, the lander separates and descends through the Mars atmosphere to the surface, encountering communication ranges from zero to several thousand kilometers. Furthermore, both the orbiter and lander possess broad-beam antennas. Hence, appreciable power may be reflected from the surface with the possibility of interference with the direct signal. Such effects are termed "multipath."

During the entry and descent phases, the reflected signal has nearly random phase and rate of change of phase due to the large relative velocities and large illumination area on the surface. The doppler shift of the reflected signal may be quite different from the direct signal because of lander and orbiter motions relative to the surface. This phenomenon can cause confusion in the orbiter as to whether a received symbol is a "mark" or a "space," since mark/space identity is keyed to the signal frequency. Multipath fading during entry may be rapid with peaks and nulls occurring in an interval shorter than a single bit time. Therefore, the received signal could be fairly constant when averaged for a period of several bit times. Changes in the average received signal level may be caused mainly by geometry variations

rather than by phased addition and cancellation with the reflected signal. In summation, entry multipath may be characterized by interference to individual bits on a random basis, and signal levels are likely to be determined by the geometry of the link. These effects are generally of a lesser magnitude than the effects present in the post-landed phase due to the increased length of the reflected signal path relative to the direct signal path during descent and entry.

After landing, the phase of the reflected signal is more predictable because the lander is fixed relative to the surface. This gives rise to a time-stationary spatial distribution of power which is a function of the lander antenna height and aspect angle (and hence the elevation angle of the orbiter). In the post-landed phase, the orbiter receives varying signal levels caused by phased addition and cancellation such that a typical periapsis pass may produce communication margin[1] as shown in Fig. 1. The envelope of these multipath variations is shown in Fig. 2.

The power reflected from the surface is a function of surface reflection coefficient, lander antenna pattern, and elevation angle. The spatial frequency of the variations is a function of antenna height and elevation angle. As the orbiter traverses the sky, it encounters the peaks and nulls of the spatial distribution, transforming them to a time distribution of signal strength. Computation of the reflection coefficient is done by classical methods for circularly polarized waves. The horizontal and vertical reflection coefficient components are computed and combined by means of the following equations:

$$|R_H| = \frac{\cos\theta_i - \sqrt{\epsilon_r - \sin^2\theta_i}}{\cos\theta_i + \sqrt{\epsilon_r - \sin^2\theta_i}} = \text{horizontal reflection coefficient}$$

$$|R_V| = \frac{\epsilon_r\cos\theta_i - \sqrt{\epsilon_r - \sin^2\theta_i}}{\epsilon_r\cos\theta_i + \sqrt{\epsilon_r - \sin^2\theta_i}} = \text{vertical reflection coefficient}$$

θ_i = angle of incidence

ϵ_r = relative permittivity of Mars surface

[1]Communication margin is defined in specification ID-3703101, *Viking* Orbiter System to Lander System Interface Requirement Document, par. 3.3.10, Langley Research Center, *Viking* '75 Project. It is essentially a measure of the received signal level relative to that level which produces a bit error rate of 0.003 in the detected data stream.

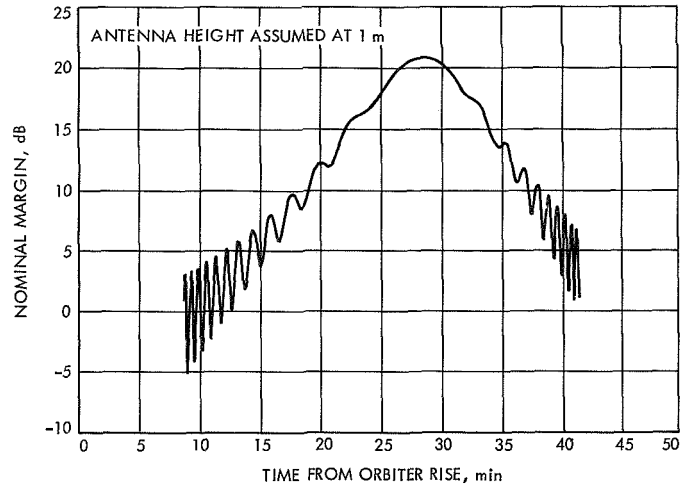

Fig. 1. Relay link performance margin versus time

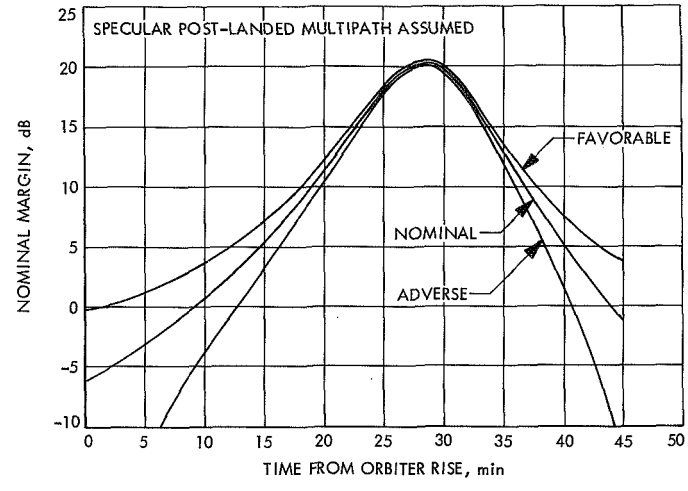

Fig. 2. Relay link performance margin versus time showing post-landed multipath envelope

$$|R_T| = \sqrt{\frac{|R_H|^2 + |R_V|^2}{2}} = \text{total reflection coefficient}$$

Assuming a relative permittivity of 3.0 for the surface of Mars (Refs. 1 and 2) the reflection coefficient can be plotted versus incidence angle as in Fig. 3.

The spatial distribution of power is computed by vectorally combining the electric fields of the direct and reflected waves with the proper amplitude and phase relationships. Assuming the free space lander antenna pattern is as shown in Fig. 4, and an antenna height of

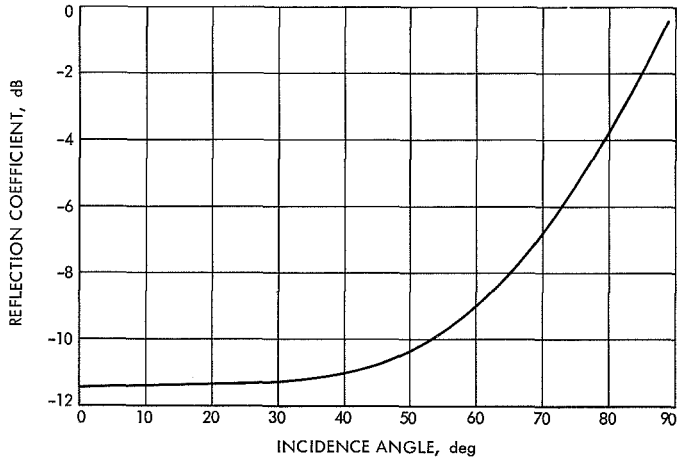

Fig. 3. Reflection coefficient $|R_T|$ as a function of incidence angle

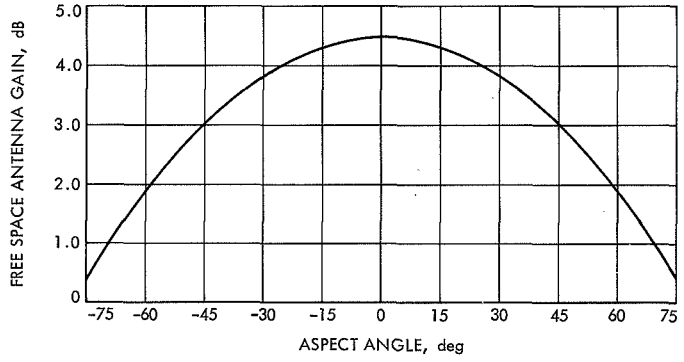

Fig. 4. Estimated lander free space antenna pattern

1 m, the spatial multipath variations (relative to the direct wave distribution) can be computed by the below equation:[2]

$$M_L = \frac{\text{received power including multipath effect}}{\text{received power without multipath effect}}$$

$$M_L = 1 + \frac{|R_T|^2 \cdot g(\pi - \theta_i)}{g(\theta_i)} - 2 \cdot |R_T| \times \sqrt{\frac{g(\pi - \theta_i)}{g(\theta_i)}} \cos\left(\frac{4\pi h}{\lambda \cos\theta_i}\right)$$

$g(\theta_i)$ = lander antenna power gain with an aspect angle of θ_i

$|R_T|$ = surface reflection coefficient at an incidence angle of θ_i

h = lander antenna height, m

λ = lander transmission wavelength, m

θ_i = incidence angle = aspect angle of lander antenna

The effective transmitting pattern (including multipath) then appears as in Fig. 5. Considering a synchronous orbit, with typical orbit parameters for *Viking*, yields the signal strength variations encountered by the orbiter as displayed in Figs. 1 and 2. The frequency of these variations is termed the "multipath lobing frequency" and is plotted versus time in Fig. 6. This figure

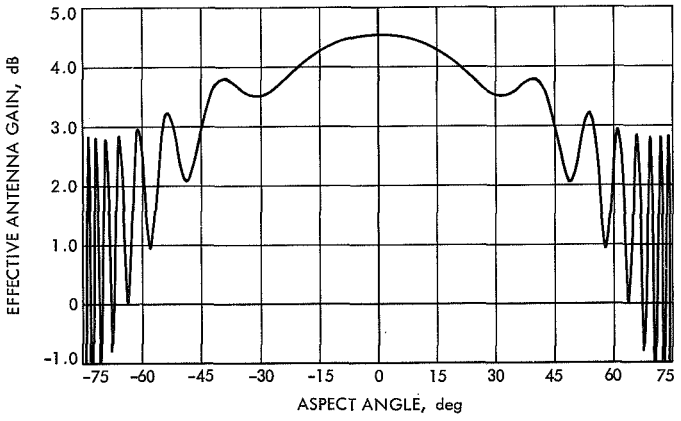

Fig. 5. Effective lander post-landed antenna pattern

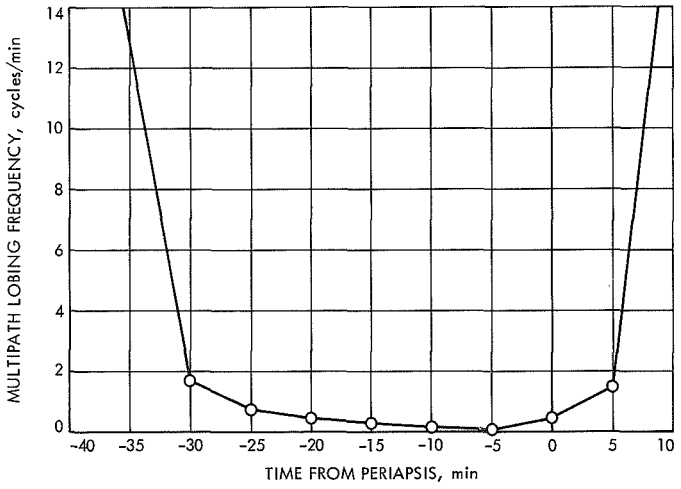

Fig. 6. Multipath lobing frequency versus time for a typical *Viking* orbit

[2]The derivation of M_L has been outlined in *Viking Relay Link Post-Landed Multipath Losses*, by G. E. Wood, Jan. 21, 1970; a correction was incorporated in the same document and issued on Feb. 4, 1970, (JPL internal publication).

essentially shows the time domain frequency of the "wiggles" in performance shown in the margin curves.

All the above presumes a specular reflecting surface on the planet. Such an assumption is valid if the surface in the local vicinity of the lander does not possess objects (rocks, rifts, rills) with rms variations greater than 1/16 wavelength from the mean surface. This means the analysis would be valid for baseball-size objects strewn randomly about the surface of the planet. Larger variations in the surface tend to smooth over the multipath effects but the envelope curves of Fig. 2 remain valid.

3. Objectives

The objectives in performing multipath simulation are threefold. Specifically the simulation effort should:

(1) Verify link performance using the multipath model described above.

(2) Provide operational norms of the functional breadboard equipment with comparisons to theoretical performance.

(3) Aid in developing a viable beacon strategy, including lock detector statistics and threshold calibrations.

4. Test Configuration

The test configuration will include equipment to simulate both the direct and reflected signals. The connection of the equipment will be as shown in Fig. 7. All equipment, other than the relay radio subsystem (RRS) and relay telemetry subsystem (RTS) breadboards, is contained within the Applied Communications Development Laboratory at JPL. All operations during testing are controlled by an XDS 930 computer. The binary data source is a pseudorandom sequence generator. Output status variables from the test are multiplexed and fed back to the computer for formatting. The detected data stream is also returned for comparison with the original data and detection of bit errors. Testing with this configuration will proceed through early 1971.

In Fig. 7 the data source modulates two FM transmitters producing the direct and reflected FSK uplink signals. Individual doppler frequency offsets can be added to the signals by combining a voltage offset to the data stream prior to modulation. Relative amplitude of the two signals can be set by multiplying the two signals independently with computer-generated functions. Finally, the signals are added together, combined with noise to establish the desired values of S/N_0, and translated to 30 MHz. This 30-MHz signal is fed directly into the IF stages of the orbiter RRS breadboard. The relative time delay of the two signal paths is established by the computer prior to modulation and can be set from 0 to 8 bit times with a resolution of 1/64 bit.

Software for test discipline via the XDS 930 computer is developed in three phases. Magnetic tapes containing trajectory parameters and link variables are prepared by the Martin-Marietta Corp. and JPL. An intermediate program at JPL converts these tapes to new tapes by abridging, scaling and formatting. The intermediate tapes are processed in the Applied Communications Development Laboratory, and a final tape is written for use with the XDS 930 computer and test fixture. Contents of the final tape are blocks of data spaced equally

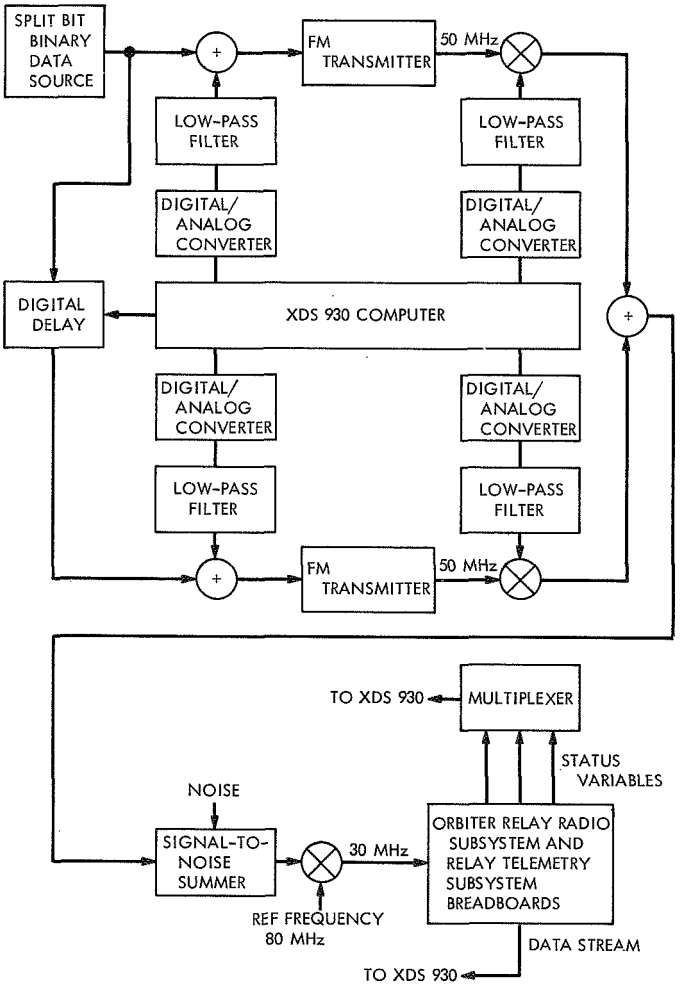

Fig. 7. Test configuration for *Viking* relay link multipath simulation with substitute lander equipment

in time. Each block contains the five parameters necessary for a link simulation point, namely:

(1) Relative strength of the direct signal.

(2) Relative strength of the reflected signal.

(3) Direct signal doppler shift.

(4) Reflected signal doppler shift.

(5) Time delay of the reflected signal.

The data blocks are spaced equally in time (generally 0.5 to 1.0 sec between blocks) and are used by the computer to construct a real-time simulated multipath environment.

References

1. NASA LRC-VPO M75-125-0, *Mars Engineering Model*, Langley Research Center, *Viking* 75 Project Office, Hampton, Va., March 13, 1970.

2. NASA SP-8020, "Mars Surface Models (1968)," *NASA Space Vehicle Design Criteria (Environment)*, May 1969.

C. Sun Occultation Logic and Sun Sensor Null Detector, *Spacecraft Control Section*

1. Introduction

During the orbit of Mars by the *Viking* orbiter the Sun will periodically be occulted. The circuit design for automatic sensing of occultation and the associated logic is presented here (see SPS 37-64, Vol. I, pp. 31–34).

2. Discussion

The *Viking* spacecraft will be put under inertial control in three axes, by either a central computer and sequencer sun occultation signal (CCSOC) or an automatic sun occultation signal (ASOC). A direct command, DC-24, will determine which signal has control. The ASOC signal is generated when there is a coincidental absence of sun gate and sun-sensor error voltage. The null detector output indicates null for offset angles less than 2 deg. A sun-gate signal is present at offset angles less than about 5 deg. CCSOC does not require the loss of sun gate to place the spacecraft under inertial control. This gives more flexibility to this command, allowing its use in possible failure modes.

When possible, the gyros are allowed to warm up before the inertial mode is initiated; however, the resultant error is minimal when there is no warm-up. There is no delay in going to inertial as a result of ASOC, whereas CCSOC inertial has a delay.

One ambiguity is that ASOC could be issued when the spacecraft is 180 deg from the normal sun orientation. This occurrence is prevented during the initial sun acquisition, by making one of the conditions for ASOC enable the receipt of the command that turns on the Canopus tracker. The Canopus tracker is turned on after sun acquisition. This, also, effectively takes care of the situation prior to shroud ejection. The probability of an erroneous ASOC signal at other times in the mission is extremely small. If it does occur, the inertial mode can be countermanded by a direct command.

Figure 1 shows the sun sensor null detector circuit. The output of this circuit is "anded" with the sun gate (null • S.G.) to form ASOC. The first amplifier serves as an absolute value amplifier through the use of steering diodes. The external roll-off capacitor provides some noise immunity. The output is 3 dB down at 1.6 Hz. The second amplifier is a level detector. The positive feedback adds hysteresis, which further reduces the possibility of chatter.

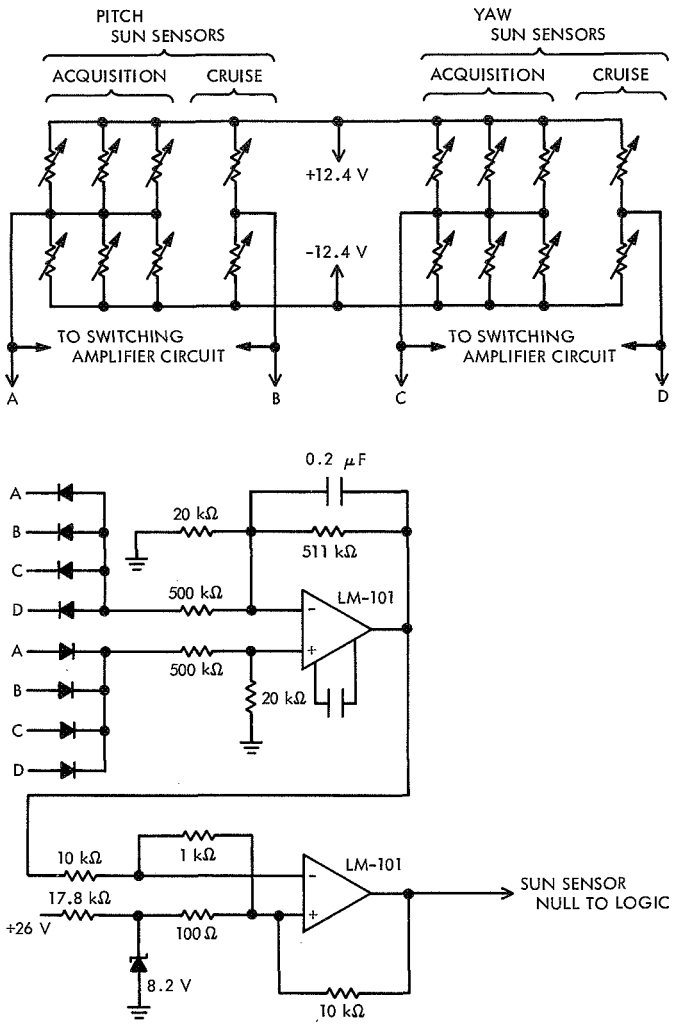

Fig. 1. Sun sensor null detector circuit

D. Articulation Control Subsystem, *Spacecraft Control Section*

1. Introduction

An articulation control subsystem has been proposed for the *Viking* spacecraft. Similar subsystems, whose prime function is the articulation of bodies on spacecraft are combined into a single subsystem. This report describes the design of a stepper motor control system that offers an excellent opportunity for a substantial hardware savings by multiplexing or time-sharing a major portion of the circuitry among the various functions in the subsystems. This is possible without any degradation of accuracy or performance. Two similar designs are being evaluated, the only difference is the error-correction technique. One employs an error-actuated constant rate mechanization, while the second corrects continuously, using a rate proportional to the error amplitude. A discussion of the systems functional elements and the results of an error analysis are contained herein.

2. Description

Figure 1 is a functional diagram of the constant-rate multiplexed stepper motor control system. It shows the analog feedback signals multiplexed into a single high-input impedance, unity gain buffer amplifier and the digital output of the up-down counter shared among the driver circuits. A serial input command, containing signal selection and output position information, is decoded. This updates the binary register and enables the appropriate multiplexer switches. Corrective action is initiated by the presence of an error at the system summing junction. If the error is greater than the threshold of the error detector, the detector will energize the clock, and depending on the polarity of the error, issue a count-up or count-down signal to the counter. Since the counter flip-flops actuate the motor drivers, the feedback signal is corrected at the rate of one step per clock pulse until the error signal is reduced to a level below the threshold of the error detector. When this occurs the error detector inhibits the clock and the system is inoperative.

Figure 2 is a diagram of the 10-bit digital-to-analog converter (D/AC) and error detector. The D/AC uses a deposited thick-film resistor network on a 1-in.^{2} substrate. The network contains a 12-bit 20-kΩ R-2R ladder and three application resistors and exhibits a maximum output voltage ratio error of ±122 ppm (±0.012%) over the temperature range of −55°C to +125°C. The use of this network virtually eliminates the ladder and summing resistors as sources of error.

The D/AC switches, which alternately switch $+V_{ref}$ or $-V_{ref}$ to the ladder network, use transistors, operated in the inverted mode. In this mode they exhibit offset voltages ≤ 0.8 mV and saturation resistances of $\leq 8\ \Omega$. While the percentage change of these parameters with temperature is equal to a normal connected transistor, the absolute change is much smaller due to the low initial values. Since high-speed operation is not required, the errors due to these temperature associated drifts were further minimized by raising the impedance level of the ladder to $R = 20$ kΩ.

The error detector consists of two integrated circuit comparators with positive and negative thresholds set by resistor dividers. Whenever the error signal is less than the thresholds, the outputs of both comparators are at ground, driving the clock inhibit signal true. If the error exceeds these limits, corrective action is initiated.

Normally in a D/AC the reference voltages are generated from tightly regulated low-drift precision supplies. However, in this design, the feedback potentiometer will be excited by the same supplies as the ladder, causing their output voltages to track on a volt/volt basis. This allows the requirements of the reference supplies to be very loose. In fact, open-loop unregulated supplies will be used.

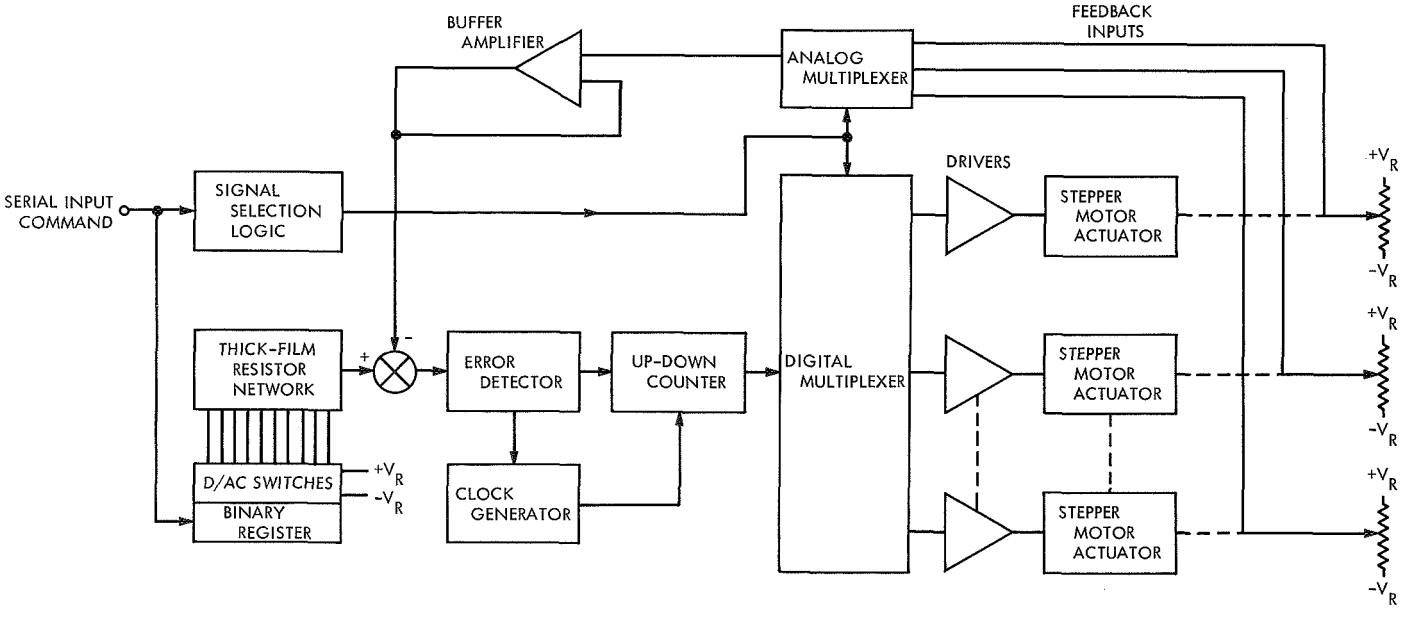

Fig. 1. Multiplexed stepper motor control system

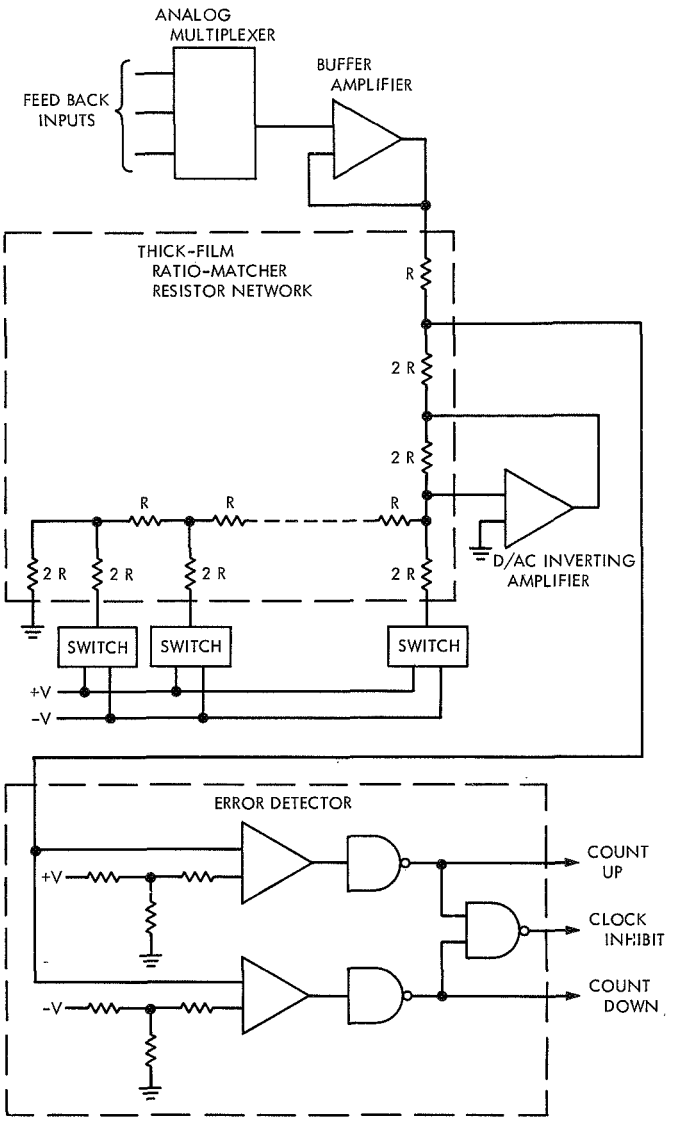

Fig. 2. 10-Bit D/AC and error detection

This equipment requires an initial adjustment, as all precision equipment does. During assembly, the threshold setting resistors will be selected to null the initial offsets with a resolution of ± 0.5 mV. This adjustment effectively reduces these errors to a negligible amount.

The logic portion of the system, which includes the 2-bit up-down counter, the 10-bit serial-to-parallel converter, and the clock generator, has not been finalized. However, the requirements for these functions are not severe, and no difficulties are anticipated.

Figure 3 is a functional diagram of the continuous error correction technique that is also being considered. It consists of an integrator, positive and negative level detectors, and a pair of reset switches. If an error current exists, the integrator output voltage will be a ramp, its direction depending on the polarity of the error current and its rate on the magnitude. When the output voltage reaches the threshold established by a resistor divider, the comparator changes state turning the reset switch (Q_1 or Q_2) on. The switch saturates, drives the noninverting input to ground and supplies reset current to the integrator summing junction. When the integrator output, which is being driven toward ground, reaches zero, the comparator again changes state, turning the reset switch off. The cycle then repeats itself. The output waveforms of Q_4 or Q_5 will be a pulse, its width equal to the reset time and its frequency dependent on

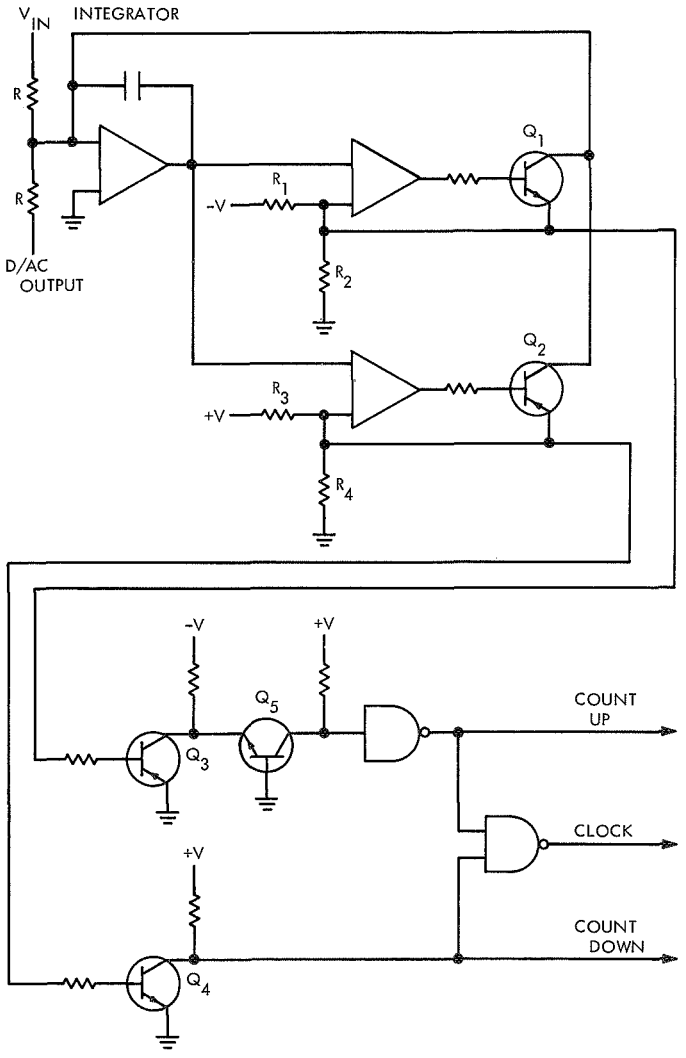

Fig. 3. Continuous error detector

the magnitude of the error signal. This signal is supplied to the counter and the motor switches and is used as a system clock. The pulse width can be varied by adjusting the impedance level of resistor combination R_1, R_2 and R_3, R_4 and thereby eliminating the need for a pulse-shaping one-shot multivibrator.

The choice between the two techniques is one of fast response, with a $\pm 0.02\%$ deadband, for the error-actuated system versus a very fine null with no deadband, but sluggish response about null for the continuous system. Both will be evaluated further.

The results of an error analysis, excluding the error contribution of the feedback potentiometer, indicates that the $\pm 3\text{-}\sigma$ error is ± 3.66 mV or $\pm 0.030\%$ full scale as compared to the worst case error of ± 6.29 mV or $\pm 0.052\%$ full scale. In the error-actuated system these numbers represent the accuracy of the null about the deadband, while for the continuous system it represents the accuracy about the command position. For either technique the accuracy is very satisfactory.

E. Separation Interfaces, *Advanced Projects Development Section*

1. Introduction

The two orbiter separation interfaces discussed in this section are the spacecraft/*Centaur* adapter and the orbiter/lander adapter interfaces. Each separation interface consists of four dual-squib release-nut mechanisms that provide the structural load path across the four interface hardpoints and four caged stroke spring assemblies that provide the separation force.

2. Release Nut Separation

The release nut mechanism (Fig. 1) consists of three threaded nut segments, separator and locking pistons, base flange, and outer casing. The three nut segments mate with a high-strength ½-20 UNF bolt allowing the assembly to be torqued to a specified preload. When the squibs are fired (Fig. 2), the separator and locking pistons are driven away from the squibs. The locking piston geometry is such that the nut segments can then be displaced radially away from the bolt by the separator piston. This reduces the preload to zero and allows the bolt to be withdrawn from the release-nut mechanism. A guide hole in the base flange that is integral with the outer casing keeps the bolt from engaging the nut segments as the bolt is withdrawn.

The structural analyses conducted to date have indicated that the required preload for each release nut at

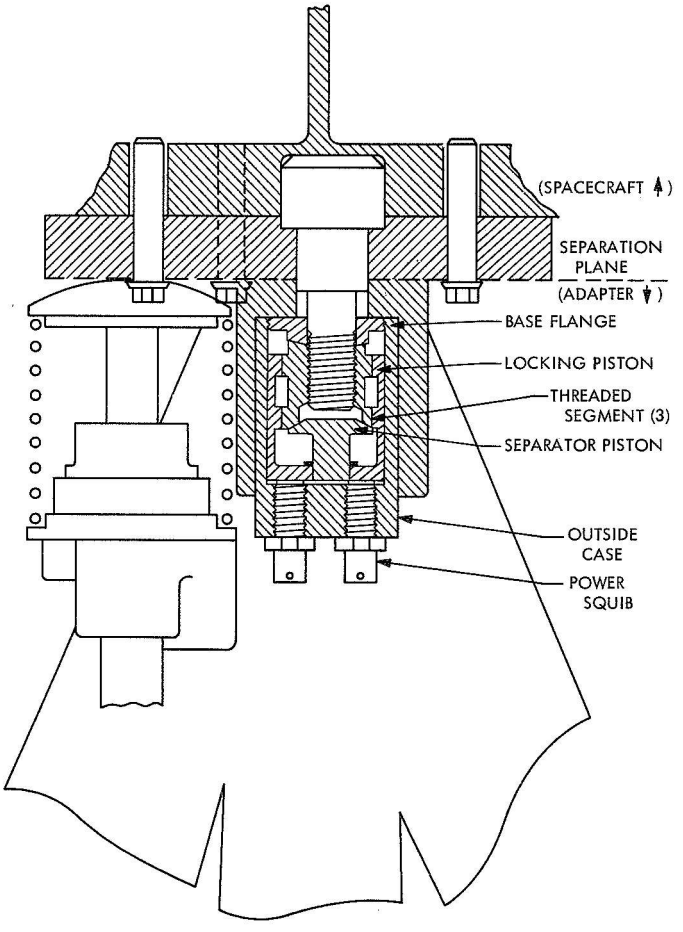

Fig. 1. Spacecraft contour adapter interface

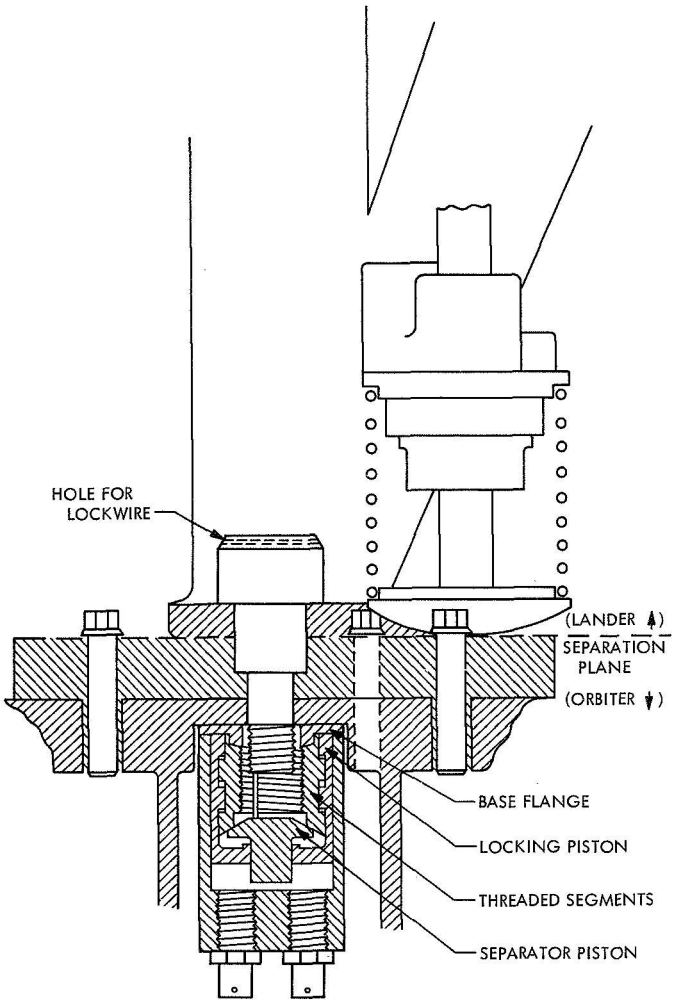

Fig. 2. Orbiter/lander adapter interface

either interface is 15,000 lb (tension/compression). Shear loads are carried by the bolt and transfer plate (as explained in *Subsections 4* and 5) and do not directly bear on the release nut.

3. Separation Springs

Four caged stroke (preloadable) helical spring assemblies provide the separation force for either interface. The caged stroke design used on *Mariner* missions will be modified to accommodate the *Viking* preload requirements. Preloadable spring assemblies are used to reduce the relative rotation during separation between the separating bodies, caused by free spring system errors, principal axis misalignment, and tolerance errors.

The springs for the spacecraft/*Centaur* adapter interface must separate a spacecraft that is partially nestled inside the *Centaur* adapter and extends 5 ft below the separation plane. Spring sizing or separation rate for this interface is determined along with other factors by the *Centaur* residual rate, initial configuration clearance between the spacecraft and *Centaur* adapter and propellant off-loading. Preliminary dynamic separation analyses have indicated the spacecraft/*Centaur* adapter separation rate to be about 2.0 ft/sec.

The orbiter/lander adapter interface separation rate is determined by the design requirement that the spring system be capable of separating the lander and adapter (if the lander does not separate) or separating just the lander adapter. In addition, the separation rate is limited by the acceleration and force loading the lander adapter and capsule can withstand. The current separation rate ranges from 1 to 2.5 ft/sec.

4. Spacecraft/*Centaur* Interface

The release nut mechanism is integrated into the spacecraft/*Centaur* adapter interface by using a transfer plate (Fig. 2). The transfer plate allows the release nut and bolt along with the caged stroke spring assembly to be preloaded prior to mating of the spacecraft with the adapter. The transfer plate is bolted to the spacecraft bus after preloading and remains with the spacecraft when separation occurs. The release nut and spring assembly remain with the adapter after separation. With the release nut on adapter side of the interface, the squib current is supplied by the *Centaur*; thus squib current transfers across the separation interface are avoided.

5. Orbiter/Lander Interface

A similar configuration to the Fig. 1 assembly is used for the orbiter/lander adapter interface except that the release nut is on the orbiter side of the interface (Fig. 2). The mating bolt and the caged stroke spring assembly are installed on the adapter side and will remain with the adapter after separation. Actuation of the release nut at this interface is achieved by power sources aboard the orbiter. This avoids transferring squib current across the interface (from the orbiter to adapter).

F. A Programmable Formater for Engineering Telemetry, *Spacecraft Measurements Section*

1. Introduction

Previous *Mariner* spacecraft have used engineering data commutators which produced fixed data formats. These data formats were fixed in both length and content (SPS 37-55, Vol. II, p. 63). This experience has indicated a well-founded need for a random access commutator which could be controlled by a reprogrammable sequencer. This type of system could potentially maximize the bandwidth usage for different mission phases, perform diagnostics on one or more subsystems in the case of isolated failures, and program around certain types of failures in the data system itself.

There is a need for efficient usage of data space in the *Viking* mission due, in part, to the large number of different engineering measurements. To efficiently use the data link, various subsets of the total telemetry measurement list should be programmed into the format at the time they are of interest. The design which follows provides a vehicle by which this may be efficiently accomplished. This design is concerned only with a portion of the total logic used to form the engineering data format. The inputs to this logic are bit sync, word sync, coded commands (to change memory contents), mode change levels, and micro-timing used for memory operation. The output of this logic is an 8-bit digital word used to select the channel which is to be sampled for the next engineering data word. The 8-bit word defines one of 256 possible channels. These channels fall into two classes, viz, those which are analog engineering inputs and those which are digital engineering inputs. When an analog input is defined, the actions which result are a switching of the analog voltage into the analog/digital converter (A/DC) input, a 7-bit conversion to digital, a dumping of the resultant 7 bits into an output shift register, and shifting of each bit serially into the data stream. When a digital input is defined, the actions which result are: shifting of the data word into the flight data subsystem (FDS) (if required), dumping of the bits into an output shift register, and shifting of each bit serially into the data stream. In the design for *Viking*, approximately 210 of the inputs are analog and approximately 46 are digital.

2. Format Structure

The format word structure is seen in Fig. 1. For a given programmed format, 148 data sources (from the total of 256) may be seen within the structure. Words 100 and 101 are constrained to be fixed digital data sources, viz., a PN sync sequence and an index word which indicates which subcommutated words are in positions 106, 107, 126, and 127.

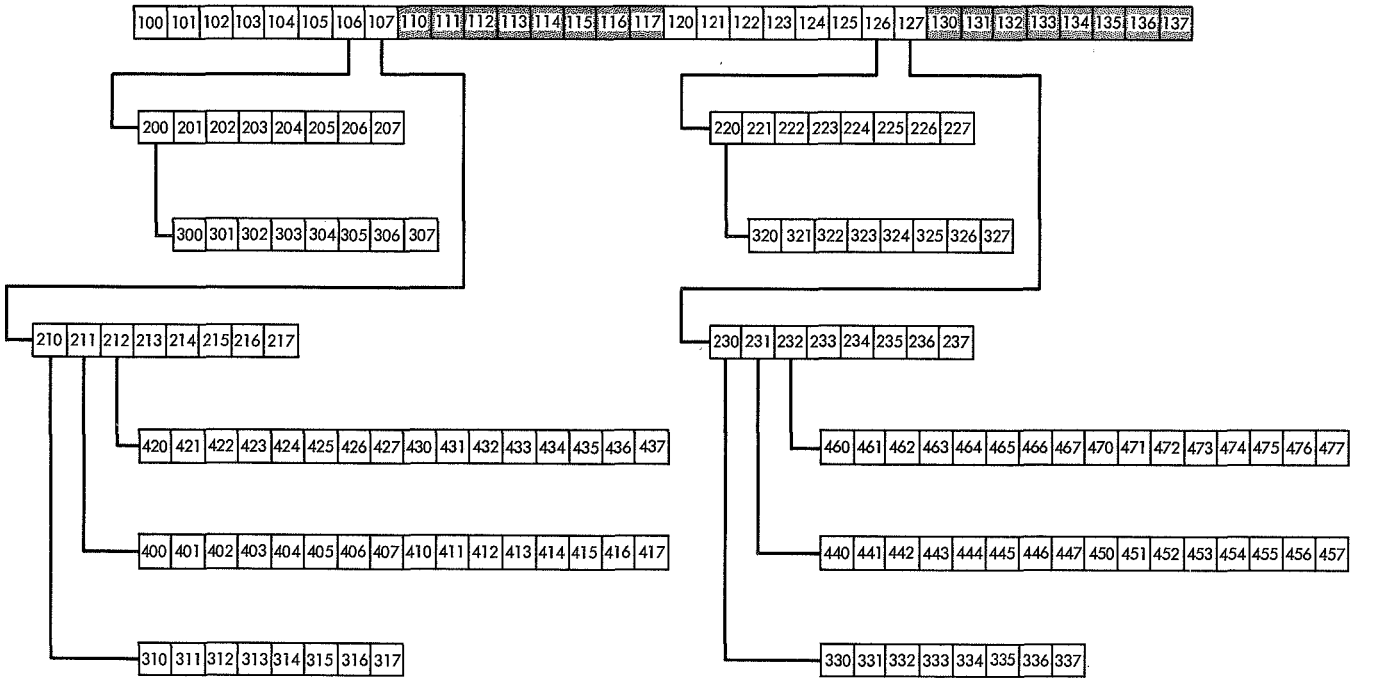

Fig. 1. Flight data subsystem engineering data format structure

A major frame (4096 words) consists of 128 minor frames (32 words). In a major frame each 400-deck position is sampled once; each 300-deck position is sampled twice; each 200-deck position is sampled 16 times; and each 100-deck position is sampled 128 times. Summarizing this in table form, over a major frame time we have:

400 deck–64 positions × 1 word/position =	64 words
300 deck–32 positions × 2 word/position =	64 words
200 deck–24 positions × 16 word/position =	384 words
100 deck–28 positions × 128 word/position =	3584 words
Total: 148 positions	4096 words

The controller for sampling within this structure is the 4096 counter (Fig. 2). A list of 148 8-bit words is stored in memory--each word representing an engineering channel for one of the 148 format positions. The 4096 counter is incremented once each format word time. The indirect address logic converts each of these counts to a memory location having a one-to-one correspondence with one of the 148 possible format positions. An 8-bit word is read out of the memory location and defines one of the 256 possible channels. The memory contents are programmed prior to launch, defining a specific subset of the 256 channels to be sampled. However, if desired, the memory may be reprogrammed via coded commands. These coded commands are entered into the memory through the "other data/memory interfaces" seen on the block diagram (Fig. 2).

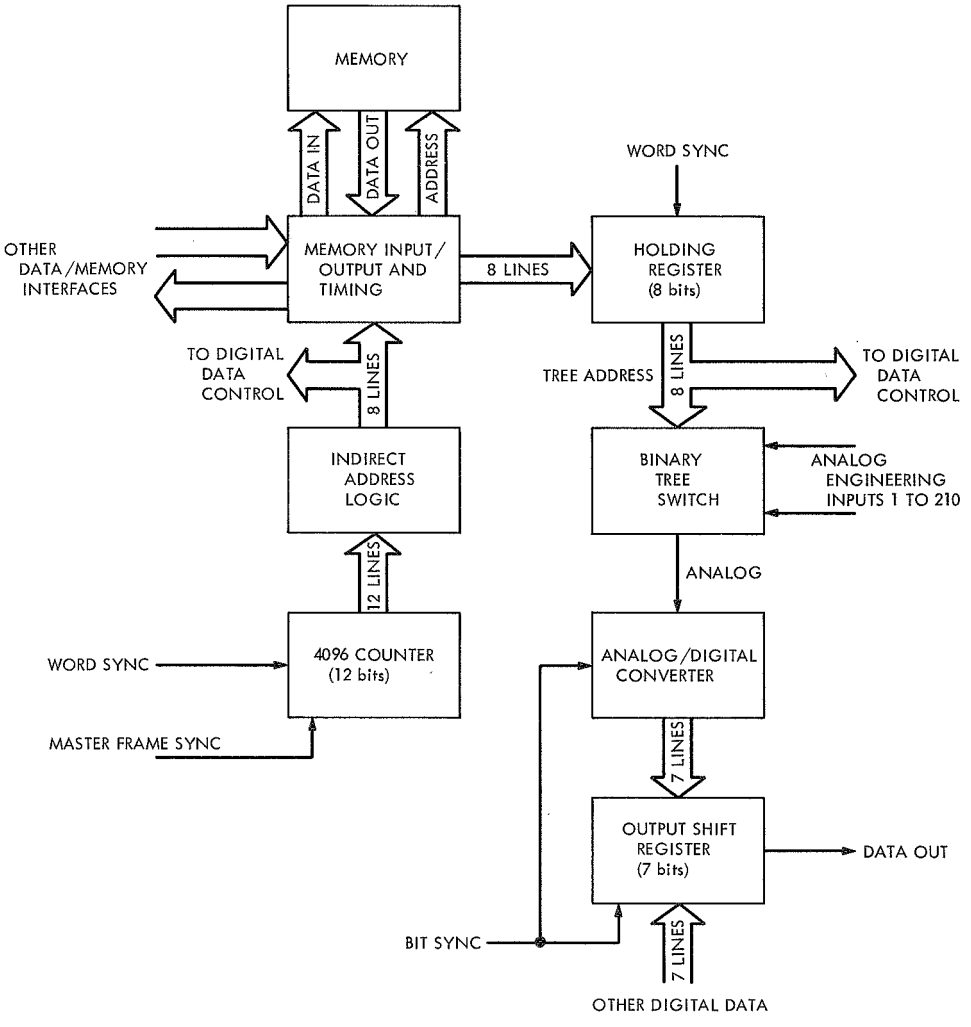

Fig. 2. Programmable format control block diagram

3. Additional System Options

Figure 3 is a block diagram of the basic system (Fig. 2) with three additional features. These are hardwired redundancy, additional memory areas, and block reprogramming.

If the "hardwired generator" (Fig. 3) output is selected by the mode control (instead of selecting the memory output), a format is generated which has the word structure in Fig. 1; however, the channel sampled at any given word in the structure is fixed. If this were used exclusively (because of memory failure), only 148 of the 256 channels would ever be sampled. A command to the FDS from the computer command subsystem (CCS) chooses either the programmable mode (memory used) or the hardwired mode.

Three additional memory areas are used in the FDS design to store three additional full-format definitions. In use the FDS have with launch, cruise, maneuver, and encounter formats stored in four separate sections of the memory. Switching from one format to another involves only a single command to the FDS. During cruise, the launch format area will be reprogrammed with a second encounter format via coded commands.

In order to facilitate diagnostics on single subsystems in the event of suspected failures, extra memory locations have been used to store the measurement channel addresses required. Utilizing a 5-bit command word (a, b, c, d, e), 8-word blocks may be called into the 110's positions or the 130's positions (shaded in Fig. 1). The

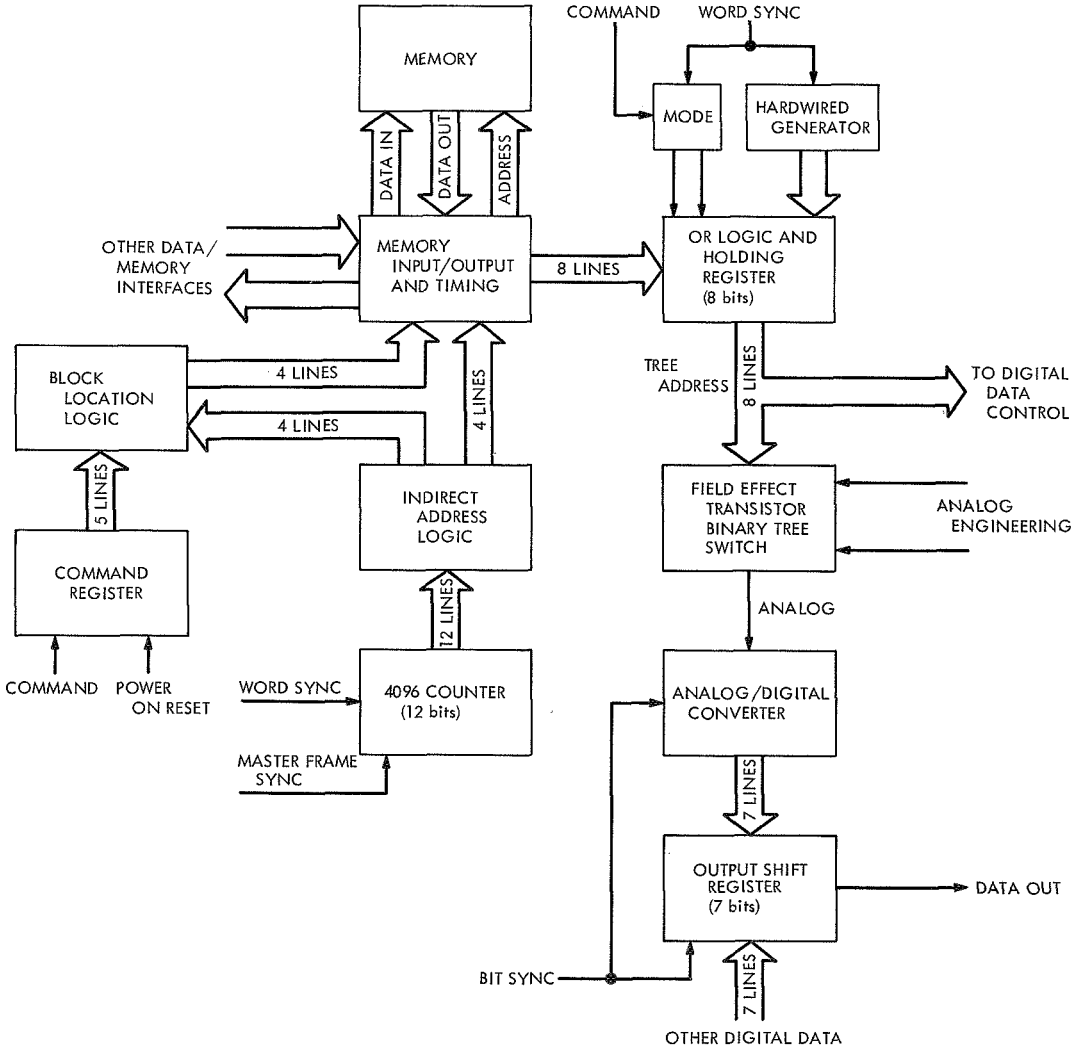

Fig. 3. Flight data subsystem engineering data format control block diagram

action resulting from any given 5-bit command is shown in Table 1. Figure 4 is a representation of word storage locations in the memory showing the extra locations used for channel addresses for subsystem diagnostics (N through Z).

4. Summary

In summary, it is seen that the full system allows three different levels of format reprogramming. The smallest reprogramming change is that of a single word in the format structure. An intermediate-size reprogramming change is that of a block of 8 words in the format structure. The largest-size reprogramming change is that of changing the complete format by moving to a different section of memory to obtain control words.

The logic for the engineering data portion of the FDS has been designed, built, and tested. The design utilized Texas Instruments 54L logic. The memory is an Electronic Memories, Inc., 8-kilobit off-the-shelf core memory. A Digital Equipment Corp. PDP-7 computer was programmed to supply coded commands to the logic through an interface rack. The computer receives the format control words and checks to see that they are correct, based on the previous coded commands which have been sent to the memory. The hardwired mode, the memory section to be used, and the 5-bit command word (a, b, c, d, e) are selectable by switches on the front panel. In the FDS these options will be controlled with coded commands. Complete checks of all logic functions have been run at room temperature and have verified the functional and logic design. In the future, checks will be run to determine the temperature and voltage margins of the hardware.

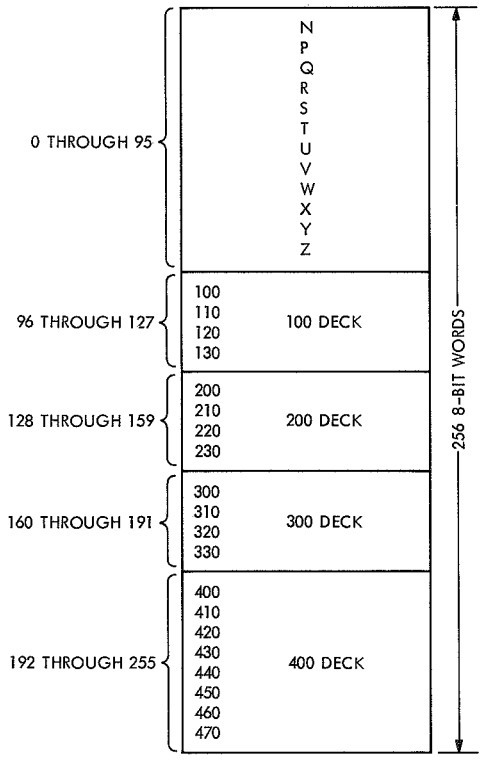

Fig. 4. Locations in segment of memory for engineering channel addresses

Table 1. Five-bit control word command sequence

Value of word in control word holding register					Substitute into 110	Substitute into 130
b	c	d	e			
0	0	0	0		N	Q
0	0	0	1		P	R
0	0	1	0		S	U
0	0	1	1		T	V
0	1	0	0		W	Y
0	1	0	1		X	Z
0	1	1	0		100	120
				Power-on-reset		
0	1	1	1	←to this state	110	130
1	0	0	0		200	220
1	0	0	1		210	230
1	0	1	0		300	320
1	0	1	1		310	330
1	1	0	0		400	420
1	1	0	1		410	430
1	1	1	0		440	460
1	1	1	1		450	470

Control word holding register				
a	b	c	d	e

If a = 0, do only second column substitution.

If a = 1, do second and third column substitutions.

When substitution is made, bits E, F, G, and J of the memory address are altered:

b is substituted for E

c is substituted for F

d is substituted for G

e is substituted for J

Bits H, K, L, and M of the memory address remain the same.